Journal Pre-proof

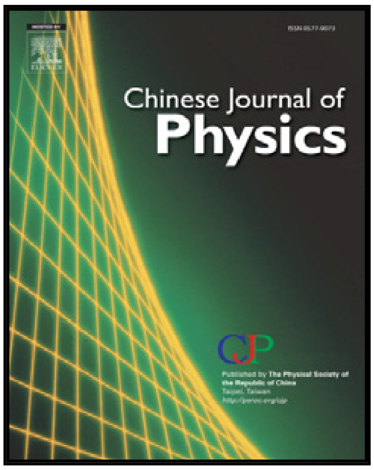

Hybrid nanofluid flow induced by an exponentially shrinking sheet

Iskandar Waini , Anuar Ishak , Ioan Pop

PII: S0577-9073(19)31016-0
DOI: https://doi.org/10.1016/j.cjph.2019.12.015
Reference: CJPH 1038

To appear in: *Chinese Journal of Physics*

Received date: 21 October 2019
Revised date: 3 December 2019
Accepted date: 18 December 2019

Please cite this article as: Iskandar Waini , Anuar Ishak , Ioan Pop , Hybrid nanofluid flow induced by an exponentially shrinking sheet, *Chinese Journal of Physics* (2019), doi: https://doi.org/10.1016/j.cjph.2019.12.015

Hybrid nanofluid flow induced by an exponentially shrinking sheet

Iskandar Waini[a,b], Anuar Ishak[b*], Ioan Pop[c]

[a]Fakulti Teknologi Kejuruteraan Mekanikal dan Pembuatan, Universiti Teknikal Malaysia Melaka, Hang Tuah Jaya, 76100 Durian Tunggal, Melaka, Malaysia

[b]Department of Mathematical Sciences, Faculty of Science and Technology, Universiti Kebangsaan Malaysia, 43600 UKM Bangi, Selangor, Malaysia

[c]Department of Mathematics, Babeş-Bolyai University, 400084 Cluj-Napoca, Romania

Highlights

- The hybrid nanofluid flow induced by an exponentially shrinking sheet is studied.
- The governing equations of the problem are transformed to the similarity equations.
- The problem is solved numerically using the boundary value problem solver (bvp4c) available in Matlab software.
- It is found that dual solutions exist for a certain range of the mass flux and stretching/shrinking parameters.
- A temporal stability analysis is performed to determine the stability of the dual solutions.

Abstract

The flow and heat transfer induced by an exponentially shrinking sheet with hybrid nanoparticles is investigated in this paper. The alumina (Al_2O_3) and copper (Cu) nanoparticles are suspended in water to form Al_2O_3-Cu/water hybrid nanofluid. In addition, the effects of magnetohydrodynamic (MHD) and radiation are also taken into account. The similarity equations are gained from the governing equations using similarity transformation, and their solutions are obtained by the aid of the bvp4c solver available in Matlab software. Results elucidate that dual solutions exist for suction strength $S > S_c$ and shrinking strength $\lambda > \lambda_c$. The critical values S_c and λ_c for the existence of the dual solutions decrease with the rising of the solid volume fractions of Cu, φ_2 and the magnetic parameter, M. Besides, the skin friction and the heat transfer rate increase with the increasing of φ_2 and M for the upper branch solutions. The increasing of radiation, R leads to reduce the surface temperature

gradient which implies to the reduction of the heat transfer rate for both branches when $\lambda < 0$ (shrinking sheet). The stability of the dual solutions is determined by the temporal stability analysis, and it is discovered that only one of them is stable and physically applicable.

Keywords Dual solutions, Exponentially shrinking sheet, Hybrid nanofluid, MHD, Radiation, Stability analysis

*Corresponding author

E-mail address: anuar_mi@ukm.edu.my (A. Ishak)

1. Introduction

Heat transfer enhancement in engineering and industrial applications has gained significant attention from the researchers for the past few years. This is because the efficiency of most equipment in this field, for example, electronic devices and heat exchangers significantly depends on the heat transfer rate. Heat transfer fluids like oil, ethylene glycol, and water limits the heat transfer rate since the thermal conductivity of these fluids are low. The deficiency of the aforementioned fluids was overcome by adding a single type of nanosized particles into the base fluids. This process was first addressed by Choi and Eastman [1] and called this mixture as 'nanofluid'. Studies have proven that nanoparticles have outstanding potentials to elevate the heat transfer rate and the thermal conductivity of the base fluids. There are numerous combinations of base fluids and nanoparticles that have been considered by the researchers such as metals (Al, Cu, Fe), metal oxides (Al_2O_3, CuO), and semiconductors (SiO_2, TiO_2) nanoparticles. The references on nanofluids are stated in the books by Das et al. [2], Minkowycz et al. [3], Shenoy et al. [4], Nield and Bejan [5], and Minea [6], and in the review papers such as Buongiorno et al. [7], Fan and Wang [8], Kakaç and Pramuanjaroenkij [9], Manca et al. [10], Sheikholeslami and Ganji [11], Myers et al. [12], and Mahian et al. [13–15]. Some interesting studies on nanofluid can be found in the literature, for example, Qayyum et al. [16] studied the effect of silver and copper nanoparticles on homogeneous-heterogeneous reactions flow with nonlinear thermal radiation. They found that the temperature of the surface enhances rapidly for silver/water than copper/water nanofluids. Furthermore, Khan et al. [17] considered the entropy generation minimization (EGM) of nanofluid flow by a thin moving needle with nonlinear thermal radiation. They considered three types of nanomaterials such as titanium dioxide, copper and aluminium oxide. The outcomes revealed that surface drag force and heat transfer enhanced linearly for higher nanoparticle volume fraction. In addition, Hayat et al. [18] examined the effects of the single-wall (SWCNTs) and the multi-wall (MWCNTs) carbon nanotubes in Marangoni convection flow with thermal radiation. It was found that the heat transfer is more effective for larger radiation and nanoparticle volume fraction parameters. Later, Hayat et al. [19] investigated the melting heat transfer and radiation effects in the stagnation point flow of carbon-water nanofluid. They found that the skin friction coefficient can be reduced for higher values of melting parameter and smaller nanoparticle volume fraction. Meanwhile, the higher cooling/heat transfer rate can be achieved for increasing nanoparticle volume fraction while the reverse behaviour is observed for higher melting parameter. The effect of silver and copper nanoparticles on the mixed convective flow of a viscous fluid induced by a rotating disk was reported by Hayat et al. [20]. It was observed that surface drag force and Nusselt number enhanced for larger nanoparticle volume fraction. Results are more obvious in the case of silver/water nanofluid when compared to copper/water nanofluid. The additional references in this direction are available in the literature, for example, Hayat et al. [21–29], Khan et al. [30–34], Farooq et al. [35], and Hsiao [36–39].

It should be mentioned that two nanofluid mathematical models introduced by Buongiorno [40] and Tiwari and Das [41] were commonly used in fluid dynamics. The Buongiorno's nanofluid model considers the Brownian motion and thermophoresis mechanisms effects in laminar fluid flow. Meanwhile, the Tiwari-Das model examines the behaviour of a nanofluid considering the solid volume fractions of the nanoparticles. However, some kind of nanofluid called 'hybrid nanofluid' were developed in order to improve the thermophysical properties of the regular nanofluid. Hybrid nanofluid contains of two or more nanoparticles with new thermophysical and chemical characteristics which believe can enhance the heat transfer rate compared to regular nanofluid due to synergistic effects (Sarkar et al. [42]). The required heat transfer effects can be achieved even for a small amount of nanoparticle volume fractions by hybridizing an appropriate combination of nanoparticles (Hemmat Esfe et al. [43]). But very few studies were reported on their preparation and synthesis because hybrid nanofluids are the new generation fluids (Sundar et al. [44]; Babu et al. [45]). Hybrid nanofluid and regular nanofluid are used in several applications such as in heating and cooling processes, cancer therapy, nanodrug delivery, power generation, and chemical processes. For further reading, comprehensive reviews on the hybrid nanofluids can be found in the review papers such as Sidik et al. [46], Akilu et al. [47], Leong et al. [48], Ahmadi et al. [49], and Huminic and Huminic [50].

In the past few years, the study on the improvement of heat transfer in a hybrid nanofluid has been investigated as a new concept in the boundary layer flow problem. For example, Devi and Devi [51] examined the flow past a permeable stretched surface with hydromagnetic effects, considering Cu-Al_2O_3/water hybrid nanofluid. In this work, the authors introduced a new thermophysical model of a hybrid nanofluid. This new thermophysical model has been verified and validated with the experimental data obtained by Suresh et al. [52], and showed an excellent correlation between the results. Then, Devi and Devi [53] extended their work to the three-dimensional flow subject to the Newtonian heating condition. They found that the heat transfer rate of hybrid nanofluid is higher than regular nanofluid. It is worth mentioning that, the stability analysis of dual solutions on the flow of a hybrid nanofluid along a shrinking surface was investigated by Waini et al. [54], and they found that only one of them is stable and physically applicable meanwhile the other is not practicable. After that, they extended this work to different surfaces such as the flow over a curved surface, nonlinear surface, and thin needle, which can be found in Waini et al. [55–57]. Later, Khashi'ie et al. [58] considered the hybrid nanofluid flow past a shrinking disc. They discovered that the heat transfer rate decelerated with the increasing values of the hybrid nanoparticle due to the higher suction strength applied on the shrinking sheet. The proposed thermophysical model has been employed by several authors to study the effect of physical parameters on the hybrid nanofluid flow, for example Hayat and Nadeem [59], Hayat et al. [60], Jamshed and Aziz [61], Yousefi et al. [62], Rostami et al. [63], Dinarvand [64], Subhani and Nadeem [65], Ahmad Khan et al.[66], and Aly and Pop [67].

Historically, the problem of steady two-dimensional flow over a linearly stretched surface was first studied by Crane [68]. Meanwhile, the occurrence of the uncommon type of flow caused by the shrinking of the sheet was first observed by Wang [69]. This type of flow is basically a reverse flow as deliberated by Goldstein [70]. In this case, a sufficient suction strength is needed to preserve the flow over a shrinking sheet as suggested by Miklavčič and Wang [71], and Fang [72]. Apart from that, the problem of flow due to a nonlinearly stretching or shrinking surface has been conducted by several researchers. The nonlinear surface is defined by its surface velocity condition whether it is in the exponential or power-law form. In this respect, Magyari and Keller [73] seem to be the first who considered an exponentially stretched surface to examine the wall temperature distribution on the flow and heat transfer characteristics. They found that the thickness of the thermal boundary layer decreases with increasing of the temperature distribution parameter for any fixed Prandtl number. This means the surface temperature gradient increases which implies the acceleration of the heat transfer occurs at the surface. Then, Elbashbeshy [74] discussed a similar problem but in the presence of wall mass suction. They noticed that the presence of suction enhanced the heat transfer and the skin friction coefficients. Also, they stated that the suction can be used as a means for cooling the moving continuous surface. After that, this problem was studied by several researchers, considering various physical parameters. For example, El-Aziz [75] studied the viscous dissipation effects on a micropolar fluid. The author discovered that an increase in the micropolar parameter led to a faster rate of cooling of the sheet for forced convective flow, while the viscous dissipation effect reduced the heat transfer rate. In addition, the effect of thermal radiation was considered by Sajid and Hayat [76], and Bidin and Nazar [77], and the problem was solved using the homotopy analysis method (HAM) and the Keller-box method, respectively. Meanwhile, Bhattacharyya and Pop [78], and Nadeem et al. [79] studied this problem under the magnetic field environment. Then, Ishak [80] and Mabood et al. [81] considered both magnetic field and thermal radiation. They found that the effect of the magnetic and radiation parameters were to reduce the local heat transfer rate at the surface for a fixed value of Prandtl number. Moreover, the nanofluid flow was studied by Zaib et al. [82], and Ghosh and Mukhopadhyay [83]. In these studies, the authors examined the nanoparticle effects on flow and heat transfer over an exponentially shrinking sheet. They found that the thermal boundary layer thickness increased, which means the heat transfer rate decreased with the rise in the nanoparticle volume fraction due to the shrinking sheet. Furthermore, some important studies in this direction can be found in the papers such as Hafidzuddin et al. [84], Partha et al. [85], Pal [86], Rohni et al. [87], Bhattacharyya [88], Sharma et al. [89], and Krishnamurthy et al. [90].

Therefore, the aim of the present paper is to examine the hybrid nanoparticle effects on the fluid flow and heat transfer induced by an exponentially stretching/shrinking sheet. Here, we consider the alumina (Al_2O_3) and copper (Cu) as hybrid nanoparticles. Then, these nanoparticles are suspended in water to form Al_2O_3-Cu/water hybrid nanofluid. The magnetohydrodynamic (MHD) and radiation effects are also taken into account. The present numerical results are compared with those of previously published data for validation purposes.

2. Mathematical model

Consider a steady two-dimensional flow induced by an exponentially stretching/shrinking sheet in a hybrid nanofluid. As illustrated in Fig. 1, the *x*- axis is along the surface and the *y*-axis is normal to it. The surface velocity is taken as $u_w(x) = U_0 e^{x/L}$, where U_0 is constant and L is the characteristic length of the sheet. The variable magnetic field $B(x) = B_0 e^{x/2L}$ is imposed along the *y*-axis where B_0 is the constant magnetic strength. Also, we assume that the nanoparticles size is uniform, and the agglomeration of nanoparticles is ignored because the hybrid nanofluid is synthesized as a stable compound.

The governing equations of the hybrid nanofluid by employing the usual boundary layer approximations are written as (see Waini et al. [56]; Ishak [80]; Bhattacharyya [88]):

$$\frac{\partial u}{\partial x} + \frac{\partial v}{\partial y} = 0 \qquad (1)$$

$$u\frac{\partial u}{\partial x} + v\frac{\partial u}{\partial y} = \frac{\mu_{hnf}}{\rho_{hnf}}\frac{\partial^2 u}{\partial y^2} - \frac{\sigma_{hnf}}{\rho_{hnf}}B^2 u \qquad (2)$$

$$u\frac{\partial T}{\partial x} + v\frac{\partial T}{\partial y} = \frac{k_{hnf}}{(\rho C_p)_{hnf}}\frac{\partial^2 T}{\partial y^2} - \frac{1}{(\rho\, C_p)_{hnf}}\frac{\partial q_r}{\partial y} \qquad (3)$$

subject to:

$$\begin{aligned} &v = v_w, \quad u = \lambda u_w, \quad T = T_w = T_\infty + T_0 e^{x/2L} \quad \text{at} \quad y = 0 \\ &u \to 0, \quad T \to T_\infty \quad \text{as} \quad y \to \infty \end{aligned} \qquad (4)$$

where u and v represent the hybrid nanofluid velocity components along the x- and y- axes. Here, v_w, T, T_w, T_∞, T_0, q_r, and λ represent the variable mass flux velocity, the hybrid nanofluid temperature, the variable surface temperature, the constant ambient temperature, the constant which measures the rate of surface temperature, the radiative heat flux, and the stretching/shrinking parameter, respectively. Note that, the sheet is stretched when $\lambda > 0$, shrunk when $\lambda < 0$ and static when $\lambda = 0$.

Using Rosseland [91] approximation, the radiative heat flux is simply expressed as follows (see Cortell [92]; Magyari and Pantokratoras [93]):

$$q_r = -\frac{4\sigma^*}{3k^*}\frac{\partial T^4}{\partial y} \qquad (5)$$

where σ^* and k^* denote the Stefan-Boltzmann constant and the mean absorption coefficient, respectively. By expanding T^4 using a Taylor series about T_∞ and disregarding the higher-order terms, we get $T^4 \cong 4\,T_\infty^3\,T - 3T_\infty^4$. Then, the energy equation (3) takes the following form (see Waini et al. [56]; Ishak [80]; Cortell [92]):

$$u\frac{\partial T}{\partial x} + v\frac{\partial T}{\partial y} = \left[\frac{k_{hnf}}{(\rho C_p)_{hnf}} + \frac{16\sigma^* T_\infty^3}{3\,(\rho C_p)_{hnf} k^*}\right]\frac{\partial^2 T}{\partial y^2} \tag{6}$$

Further, ρ_{nhf}, μ_{hnf}, k_{hnf}, σ_{hnf}, and $(\rho C_p)_{hnf}$ represent the density, dynamic viscosity, thermal conductivity, electrical conductivity, and heat capacity of the hybrid nanofluid, respectively. As suggested by Devi and Devi [51], Yousefi et al. [62], Rostami et al. [63], Dinarvand [64], and Oztop and Abu-Nada [94], we are employing the equations to evaluate the thermophysical properties of the nanofluid and the hybrid nanofluid as given in Table 1. Here, φ_1 and φ_2 represent the volume fractions of Al_2O_3 and Cu nanoparticles, respectively. Meanwhile, μ, ρ, k, C_p, σ, and (ρC_p) represent the dynamic viscosity, density, thermal conductivity, specific heat at constant pressure, electrical conductivity, and heat capacity, respectively. Meanwhile, the subscripts hnf, nf, f, $n1$, and $n2$ are used to represent the hybrid nanofluid, nanofluid, fluid, Al_2O_3 and Cu solid components, respectively. Table 2 provides the nanoparticles and base fluid physical properties as in Oztop and Abu-Nada [94], and Raza et al. [95].

The similarity solutions of Eqs. (1) to (4) are obtained using the following similarity variables (see Ishak [80]; Bhattacharyya [88]):

$$\psi = \sqrt{2U_0\nu_f L}\,f(\eta)\,e^{x/2L}, \quad \theta(\eta) = \frac{T - T_\infty}{T_w - T_\infty}, \quad \eta = y\sqrt{\frac{U_0}{2\nu_f L}}\,e^{x/2L} \tag{7}$$

where the stream function ψ is defined as $u = \partial\psi/\partial y$ and $v = -\,\partial\psi/\partial x$. Using these definitions, the continuity equation (1) is fully satisfied and we have:

$$u = U_0 e^{x/L} f'(\eta), \qquad v = -\sqrt{\frac{U_0\nu_f}{2L}}\,e^{x/2L}\big(f(\eta) + \eta f'(\eta)\big) \tag{8}$$

so that:

$$v_w = -\sqrt{\frac{U_0 \nu_f}{2L}} e^{x/2L} S \tag{9}$$

Here, $f(0) = S$ is the mass flux parameter which represents the suction ($S > 0$) and injection ($S < 0$). Thus, Eqs. (2) and (3) become:

$$\frac{\mu_{hnf}/\mu_f}{\rho_{hnf}/\rho_f} f''' + f f'' - 2f'^2 - \frac{\sigma_{hnf}/\sigma_f}{\rho_{hnf}/\rho_f} M f' = 0 \tag{10}$$

$$\frac{1}{\Pr} \frac{1}{(\rho C_p)_{hnf}/(\rho C_p)_f} \left(\frac{k_{hnf}}{k_f} + \frac{4}{3} R \right) \theta'' + f\theta' - f'\theta = 0 \tag{11}$$

subject to:

$$f(0) = S, \quad f'(0) = \lambda, \quad \theta(0) = 1$$
$$f'(\infty) = 0, \quad \theta(\infty) = 0 \tag{12}$$

where the notation ($'$) means the differentiation with respect to η, and $\Pr = \mu_f (C_p)_f / k_f$ represents the Prandtl number, $M = 2\sigma_f B_0^2 L / U_0 \rho_f$ represents the magnetic parameter, and $R = 4\, \sigma^* T_\infty^3 / k^* k_f$ represents the radiation parameter. It should be noticed that the flow over a linearly shrinking sheet in a regular fluid $\varphi_1 = \varphi_2 = 0$ was considered by Fang and Zhang [96] where the authors have, in this case, established an analytical solution of their Eq. (6).

The coefficient of the skin friction C_f and the local Nusselt number Nu_x are defined as:

$$C_f = \frac{\tau_w}{\rho_f\, u_w^2}, \quad Nu_x = \frac{2L q_w}{k_f (T_w - T_\infty)} \tag{13}$$

where the shear stress τ_w and the heat flux from the surface q_w are given by (see Waini et al. [56]; Cortell [92]):

$$\tau_w = \mu_{hnf} \left(\frac{\partial u}{\partial y} \right)_{y=0}, \qquad q_w = -k_{hnf} \left(\frac{\partial T}{\partial y} \right)_{y=0} + (q_r)_{y=0} \tag{14}$$

Using (7), (13) and (14), we get:

$$Re_x^{1/2}\,C_f = \frac{\mu_{hnf}}{\mu_f} f''(0), \qquad Re_x^{-1/2} Nu_x = -\left(\frac{k_{hnf}}{k_f} + \frac{4}{3}R\right)\theta'(0) \tag{15}$$

where the local Reynolds number is expressed as $Re_x = 2Lu_w/\nu_f$.

3. Stability analysis

It is discovered that dual solutions exist from the boundary value problem (10) to (12) for a certain value of the physical parameters. Therefore, a stability analysis which first proposed by Merkin [97] is performed to determine which one of the solutions is stable. Weidman et al. [98] initiated to study the stability of the solutions by introducing a dimensionless time variable, τ in order to determine the stable solutions as time evolves. In their work, they found that the upper branch solutions are stable and thus physically relevant, meanwhile, the opposite trend is noticed for the lower branch solutions. To study the stability of the solutions of Eqs. (1) to (3), the unsteady form of these equations significantly depends. Following Merkin [97], and Weidman et al. [98], the new variables for Eq. (7) are given by:

$$\psi = \sqrt{2U_0\nu_f L}\,f(\eta,\tau)\,e^{x/2L},\ \ \theta(\eta,\tau) = \frac{T - T_\infty}{T_w - T_\infty},\ \ \eta = y\sqrt{\frac{U_0}{2\nu_f L}}\,e^{x/2L},\ \ \tau = \frac{U_0}{2L}\,t e^{x/L} \tag{16}$$

Using (16), the following equations are obtained:

$$\frac{\mu_{hnf}/\mu_f}{\rho_{hnf}/\rho_f}\frac{\partial^3 f}{\partial\eta^3} + f\frac{\partial^2 f}{\partial\eta^2} - 2\left(\frac{\partial f}{\partial\eta}\right)^2 - \frac{\sigma_{hnf}/\sigma_f}{\rho_{hnf}/\rho_f} M\frac{\partial f}{\partial\eta} - \frac{\partial^2 f}{\partial\eta\partial\tau} = 0 \tag{17}$$

$$\frac{1}{\Pr}\frac{1}{(\rho C_p)_{hnf}/(\rho C_p)_f}\left(\frac{k_{hnf}}{k_f} + \frac{4}{3}R\right)\frac{\partial^2\theta}{\partial\eta^2} + f\frac{\partial\theta}{\partial\eta} - \frac{\partial f}{\partial\eta}\theta - \frac{\partial\theta}{\partial\tau} = 0 \tag{18}$$

subject to:

$$f(0,\tau) = S, \quad \frac{\partial f}{\partial\eta}(0,\tau) = \lambda, \quad \theta(0,\tau) = 1$$

$$\frac{\partial f}{\partial\eta}(\infty,\tau) = 0, \quad \theta(\infty,\tau) = 0 \tag{19}$$

To examine the stability behaviour, the steady solution $f = f_0(\eta)$ and $\theta = \theta_0(\eta)$ of Eqs. (10) to (12) are perturbed using the following disturbance (see Weidman et al. [98]):

$$f(\eta,\tau) = f_0(\eta) + e^{-\gamma\tau}F(\eta), \quad \theta(\eta,\tau) = \theta_0(\eta) + e^{-\gamma\tau}G(\eta) \tag{20}$$

where the unknown eigenvalue is denoted by γ, while $F(\eta)$ and $G(\eta)$ are relatively small compared to $f_0(\eta)$ and $\theta_0(\eta)$. The perturbation is taken in the exponential form since it clearly shows the decay or growth of disturbance. Then, Eq. (20) is substituted into Eqs. (17) to (19), thus the following linear eigenvalue problems are obtained.

$$\frac{\mu_{hnf}/\mu_f}{\rho_{hnf}/\rho_f}F''' + f_0F'' + f_0''F - 4f_0'F' - \frac{\sigma_{hnf}/\sigma_f}{\rho_{hnf}/\rho_f}MF' + \gamma F' = 0 \tag{21}$$

$$\frac{1}{\Pr}\frac{1}{(\rho C_p)_{hnf}/(\rho C_p)_f}\left(\frac{k_{hnf}}{k_f} + \frac{4}{3}R\right)G'' + f_0G' + \theta_0'F - f_0'G - \theta_0F' + \gamma G = 0 \tag{22}$$

subject to:

$$\begin{gathered} F(0) = 0, \quad F'(0) = 0, \quad G(0) = 0 \\ F'(\infty) = 0, \quad G(\infty) = 0 \end{gathered} \tag{23}$$

The stability of the solutions is analyzed by the smallest eigenvalue γ. Following Harris et al. [99], without loss of generality, we find the smallest eigenvalue γ in Eqs. (21) to (23) for the case of $F''(0) = 1$.

4. Results and discussion

Equations (10) to (12) were solved numerically by the aid of bvp4c solver in Matlab software. This solver employs the finite difference scheme that implements the 3-stage Labatto IIIa formula. Also, the appropriate thickness of the boundary layer, η_∞ must be chosen depending on the values of the parameters applied. Here, we have taken a finite value of η_∞ in the range of $10 \le \eta_\infty \le 40$. The procedures of this method are clearly discussed by Shampine et al. [100]. Also, this outstanding solver has been broadly utilized by other researchers such as Awaludin et al. [101], Soid et al. [102], Jusoh et al. [103], Kamal et al. [104], Khashi'ie et al. [105,106], and Waini et al. [107]. To conduct this study, 0.1 solid volume fraction of Al_2O_3 ($\varphi_1 = 0.1$) is added into the base fluid (water) as suggested by Devi and Devi [51]. Consequently, several solid volume fractions of Cu ($0 \leq \varphi_2 \leq 0.04$) are added into the mixture in order to form Al_2O_3-Cu/water hybrid nanofluid.

The values of the local Nusselt number $-\theta'(0)$ for regular fluid ($\varphi_1 = \varphi_2 = 0$) when $S = 0$ and $\lambda = 1$ (stretching sheet) under different values of Pr, M, and R are presented in Table 3. Meanwhile, Table 4 describes the values of the skin friction coefficient $f''(0)$ and the local Nusselt number $-\theta'(0)$ for regular fluid ($\varphi_1 = \varphi_2 = 0$) when $\mathrm{Pr} = 0.7$, $S = 3$, $M = R = 0$, and $\lambda = -1$ (shrinking sheet). Tables 3 and 4 show the comparison of the present numerical results obtained using bvp4c solver with the existing results available in the literature for a special case of the present study. Magyari and Keller [73], El-Aziz [75], and Ghosh and Mukhopadhyay [83] adopted the shooting method, while Bidin and Nazar [77], and Ishak [80] employed the Keller box method, and Hafidzuddin et al. [84] used the bvp4c solver in their studies. The present results demonstrate an excellent agreement with those obtained by the aforesaid literature as shown in Tables 3 and 4. At the same time, numerical results presented in these tables can also represent a comparison of numerical results produced by different methods, i.e. the shooting, Keller box, and bvp4c methods. Based on the comparison, we found that the bvp4c solver produced satisfactory solutions comparable to the abovementioned numerical methods.

Moreover, the values of $Re_x^{1/2} C_f$ and $Re_x^{-1/2} Nu_x$ for Cu/water nanofluid ($\varphi_1 = 0$) and Al_2O_3-Cu/water hybrid nanofluid ($\varphi_1 = 0.1$) when $\mathrm{Pr} = 6.2$ under different values of φ_2, λ, S, M, and R are given in Table 5. Note that, the effect of φ_2, λ, and S are to enhance the heat transfer rate $Re_x^{-1/2} Nu_x$, but it decelerates the values of $Re_x^{1/2} C_f$ for both nanofluid and hybrid nanofluid. Meanwhile, the rising values of M tends to reduce the values of $Re_x^{1/2} C_f$ and $Re_x^{-1/2} Nu_x$. Moreover, the values of $Re_x^{-1/2} Nu_x$ increases with the increasing values of R, whereas the values of $Re_x^{1/2} C_f$ are not influenced by R. It is also noticed that the values of $Re_x^{-1/2} Nu_x$ for Al_2O_3-Cu/water hybrid nanofluid are greater compared to Cu/water nanofluid which implies that the hybrid nanoparticles enhance the rate of heat transfer.

From Figs. 2 to 7, we observe that the solutions of Eqs. (10) to (12) are not unique for a certain range of S and λ. No similarity solutions are obtained when $S < S_c$ and $\lambda < \lambda_c$, where S_c and λ_c are the critical values for which the solutions are in existence. For more details, Figs. 2 and 3 are provided to show the effect of S and φ_2 on the skin friction coefficient $Re_x^{1/2} C_f$ and the local Nusselt number $Re_x^{-1/2} Nu_x$ for the shrinking sheet

($\lambda = -1$) when $\Pr = 6.2, M = \varphi_1 = 0.1$, and $R = 3$. Generally, the vorticity occurs for the shrinking sheet flow. Thus, the similarity solutions do not exist since the vorticity could not be confined in the boundary layer. These figures reveal that a sufficient suction strength is needed to preserve the flow over a shrinking sheet. This finding is supported by the results obtained by Miklavčič and Wang [71], and Fang [72]. The existence of dual solutions is observed in the presence of sufficient suction strength where $S \geq S_c$. Note that, $S_{c1} \geq 2.1877$, $S_{c2} \geq 2.1259$ and $S_{c3} \geq 2.0777$ when $\varphi_2 = 0, 0.02$, and 0.04, respectively, for the dual solutions to be in existence. Moreover, for fixed value of S, the values of $Re_x^{1/2} C_f$ and $Re_x^{-1/2} Nu_x$ enhance with increasing values of φ_2 for the first solutions, but reduce for the second solutions.

The variations of $Re_x^{1/2} C_f$ and $Re_x^{-1/2} Nu_x$ against λ for different values of φ_2 when $\Pr = 6.2, M = \varphi_1 = 0.1, R = 3$, and $S = 2.4$ are illustrated in Figs. 4 and 5. The rise of φ_2 tends to reduce the values of $Re_x^{1/2} C_f$ and $Re_x^{-1/2} Nu_x$ for the second solutions. However, for the first solutions, we observe that the values of $Re_x^{1/2} C_f$ increases when $\lambda < 0$, decreases when $\lambda > 0$, and there is no skin friction when $\lambda = 0$, whereas the small increment is noticed for the values of $Re_x^{-1/2} Nu_x$ when λ is near to λ_c. This finding is consistent with the fact that the added hybrid nanoparticles improve the heat transfer rate due to synergistic effects as discussed by Sarkar et al. [42]. Based on our computation, the critical values of λ for $\varphi_2 = 0$, 0.02 and 0.04 are $\lambda_c = -1.1892$, -1.2560, and -1.3127, respectively.

Figures 6 and 7 show the effect of M on $Re_x^{1/2} C_f$ and $Re_x^{-1/2} Nu_x$ against λ when $\Pr = 6.2, \varphi_1 = 0.1, \varphi_2 = 0.04, R = 3$, and $S = 2.4$. We notice that the presence of M is to delay the separation of the boundary layer where the values of λ_c are slightly moves to the left. According to Bhattacharyya and Pop [78], this phenomenon occurs due to the fact that the Lorenz force suppressed the vorticity produced by the shrinking of the sheet inside the boundary layer. Besides, the values of $Re_x^{1/2} C_f$ and $Re_x^{-1/2} Nu_x$ increase with the increasing of M for the first solutions, but it is obviously seen when λ is near to λ_c, whereas the opposite trend is observed for the second solutions. The dual solutions are obtained for $\lambda > \lambda_c$, where the critical values for $M = 0, 0.1$, and 0.2 are $\lambda_c = -1.2482$, -1.3127, and -1.3770, respectively.

The velocity $f'(\eta)$ and the temperature $\theta(\eta)$ of the hybrid nanofluid for several pertinent parameters are displayed in Figs. 8 to 11. From these figures, we note that there exist dual solutions for the velocity $f'(\eta)$ and temperature $\theta(\eta)$ profiles which asymptotically fulfilled the infinity boundary conditions (12), thus the accuracy of the present numerical results are achieved. As shown in Figs. 8 and 9, it is observed that the rise of φ_2 leads to an increment in $f'(\eta)$ for the first solutions, and it is decreasing for the second solutions, but the observation is conversed for $\theta(\eta)$ when $M = \varphi_1 = 0.1, R = 3, S = 2.4, \lambda = -1.15$, and $\Pr = 6.2$. Similar trends are discerned in Figs. 10 and 11 for magnetic parameter M effects on $f'(\eta)$ and $\theta(\eta)$ when $\varphi_1 = 0.1, \varphi_2 = 0.04, R = 3, S = 2.4, \lambda = -1.24$, and $\Pr = 6.2$. From these figures, we observe that the velocity and the temperature gradients for the first solutions increase with the rising values of φ_2 and M which implies to the increment of the skin friction coefficient $Re_x^{1/2}C_f$ and the heat transfer rate $Re_x^{-1/2}Nu_x$ of the hybrid nanofluid. These findings are supported by the results presented in Figs. 4 to 7.

The effects of the radiation parameter R on $Re_x^{-1/2}Nu_x$ against λ when $\Pr = 6.2, M = \varphi_1 = 0.1, \varphi_2 = 0.04$, and $S = 2.4$ are displayed in Fig. 12. We found that $Re_x^{-1/2}Nu_x$ decreases for both branches in the presence of radiation when $\lambda < 0$ (shrinking sheet), which implies the reduction of the heat transfer rate at the surface. However, the rate of heat transfer increases when $\lambda > 0$ (stretching sheet) and occur almost at the same rate when $\lambda = 0$ for the first solutions. Figure 13 portrays the temperature $\theta(\eta)$ of the hybrid nanofluid for different values of R when $M = \varphi_1 = 0.1$, $\varphi_2 = 0.04$, $S = 2.4, \lambda = -1$, and $\Pr = 6.2$. We observe that the rise in R thickens the thermal boundary layer for both branches. The radiation is dominant over conduction with the increasing of R. Therefore, the temperature $\theta(\eta)$ increases due to the high radiation energy presence in the flow field. From the numerical computations, we found that $\lambda_c = -1.3127$ for all values of R.

The smallest eigenvalues γ against λ when $M = \varphi_1 = 0.1, R = 3$, and $S = 2.4$ are portrayed in Fig. 14. Referring to Eq. (20), an initial decay of disturbance occurs for the positive value of γ as $\tau \to \infty$, means that the flow is stable as time evolves. Meanwhile, an initial growth of disturbance occurs for the negative value of γ, which means the flow is unstable. As λ approaching the critical value λ_c, it is observed that γ tends to zero for both upper (stable) and lower (unstable) branches. This behaviour implies that the solutions are bifurcated at the critical values.

5. Conclusion

The flow and heat transfer induced by an exponentially shrinking sheet in a hybrid nanofluid was examined in the present paper. For validation purposes, the present results were verified with the previously published data and an excellent agreement was found between those results. Results revealed that an adequate suction strength is needed to preserve the flow over a shrinking sheet. Here, we found that the solutions of Eqs. (10) to (12) are not unique for $S > S_c$ and $\lambda > \lambda_c$. The skin friction coefficient $Re_x^{1/2} C_f$ and the local Nusselt number $Re_x^{-1/2} Nu_x$ increased with the increasing of φ_2 and M for the first solutions when λ is near to λ_c. Also, the effect of φ_2 and M are to decrease the temperature $\theta(\eta)$, but increases the velocity $f'(\eta)$ of the hybrid nanofluid for the first solutions, whereas opposite behaviours were observed for the second solutions. The reduction of the heat transfer rate was observed for both branches with the increasing values of the radiation parameter R when $\lambda < 0$ (shrinking sheet). We also observed that the rise in R thickened the thermal boundary layer for both branches. Using the temporal stability analysis, we found that only one of the two solutions is stable and thus physically applicable.

Acknowledgements

The financial supports received from the Ministry of Education Malaysia (Project Code: FRGS/1/2019/STG06/UKM/01/4) and the Universiti Teknikal Malaysia Melaka are gratefully acknowledged. The work of Ioan Pop was supported by the grant PN-III-P4-ID-PCE-2016-0036, UEFISCDI from the Ministry of Science, Romania.

Table 1 Thermophysical properties of nanofluid and hybrid nanofluid

Properties	Nanofluid	Hybrid nanofluid
Density	$\rho_{nf} = (1-\varphi_1)\rho_f + \varphi_1\rho_{n1}$	$\rho_{hnf} = (1-\varphi_2)\left[(1-\varphi_1)\rho_f + \varphi_1\rho_{n1}\right] + \varphi_2\rho_{n2}$
Heat capacity	$(\rho C_p)_{nf} = (1-\varphi_1)(\rho C_p)_f + \varphi_1 (\rho C_p)_{n1}$	$(\rho C_p)_{hnf} = (1-\varphi_2)\left[(1-\varphi_1)(\rho C_p)_f + \varphi_1(\rho C_p)_{n1}\right] + \varphi_2(\rho C_p)_{n2}$

Dynamic viscosity	$\mu_{nf} = \dfrac{\mu_f}{(1-\varphi_1)^{2.5}}$	$\mu_{hnf} = \dfrac{\mu_f}{(1-\varphi_1)^{2.5}\,(1-\varphi_2)^{2.5}}$
Thermal conductivity	$k_{nf} = \dfrac{k_{n1} + 2k_f - 2\varphi_1(k_f - k_{n1})}{k_{n1} + 2k_f + \varphi_1(k_f - k_{n1})} \times (k_f)$	$k_{hnf} = \dfrac{k_{n2} + 2k_{nf} - 2\varphi_2(k_{nf} - k_{n2})}{k_{n2} + 2k_{nf} + \varphi_2(k_{nf} - k_{n2})} \times (k_{nf})$ where $k_{nf} = \dfrac{k_{n1} + 2k_f - 2\varphi_1(k_f - k_{n1})}{k_{n1} + 2k_f + \varphi_1(k_f - k_{n1})} \times (k_f)$
Electrical conductivity	$\sigma_{nf} = 1 + \dfrac{3\left(\frac{\sigma_{n1}}{\sigma_f} - 1\right)\varphi_1}{2 + \frac{\sigma_{n1}}{\sigma_f} - \left(\frac{\sigma_{n1}}{\sigma_f} - 1\right)\varphi_1} \times (\sigma_f)$	$\sigma_{hnf} = \dfrac{\sigma_{n2} + 2\sigma_{nf} - 2\varphi_2(\sigma_{nf} - \sigma_{n2})}{\sigma_{n2} + 2\sigma_{nf} + \varphi_2(\sigma_{nf} - \sigma_{n2})} \times (\sigma_{nf})$ where $\sigma_{nf} = \dfrac{\sigma_{n1} + 2\sigma_f - 2\varphi_1(\sigma_f - \sigma_{n1})}{\sigma_{n1} + 2\sigma_f + \varphi_1(\sigma_f - \sigma_{n1})} \times (\sigma_f)$

Table 2 Thermophysical properties of nanoparticles and water

Properties	Al_2O_3	Cu	water
$\rho\ (kg/m^3)$	3970	8933	997.1
$C_p\ (J/kgK)$	765	385	4179
$k\ (W/mK)$	40	400	0.613
$\sigma\ (S/m)$	3.69×10^7	5.96×10^7	0.05
Prandtl number, Pr			6.2

Table 3 Values of $-\theta'(0)$ for regular fluid ($\varphi_1 = \varphi_2 = 0$) when $S = 0$, $\lambda = 1$ (stretching sheet) under different values of Pr, M, and R.

Pr	M	R	Magyari and Keller [73]	El-Aziz [75]	Bidin and Nazar [77]	Ishak [80]	Present results
0.5	0	0	0.594338	0.594493			0.594339
1	0	0	0.954782	0.954785	0.9548	0.9548	0.954783
2	0	0			1.4714	1.4715	1.471460

3	0	0	1.869075	1.869074	1.8691	1.8691	1.869074
5	0	0	2.500135	2.500132		2.5001	2.500132
10	0	0	3.660379	3.660372		3.6604	3.660372
1	1	0				0.8611	0.861094
1	0	1			0.5315	0.5312	0.531158
1	1	1				0.4505	0.450536

Table 4 Values of $f''(0)$ and $-\theta'(0)$ for regular fluid ($\varphi_1 = \varphi_2 = 0$) when $\Pr = 0.7$, $S = 3$, $M = R = 0$, $\lambda = -1$ (shrinking sheet)

	Ghosh and Mukhopadhyay [83]		Hafidzuddin et al. [84]		Present results	
	First Solution	Second Solution	First Solution	Second Solution	First Solution	Second Solution
$f''(0)$	2.39082	-0.97223	2.3908	-0.9722	2.390814	-0.972247
$-\theta'(0)$	1.77124	0.84832	1.7712	0.8483	1.771237	0.848316

Table 5 Values of $Re_x^{1/2}\, C_f$ and $Re_x^{-1/2} Nu_x$ for Cu/water nanofluid ($\varphi_1 = 0$) and Al_2O_3-Cu/water hybrid nanofluid ($\varphi_1 = 0.1$) when $\Pr = 6.2$ under different values of φ_2, λ, S, M, and R

φ_2	λ	S	M	R	Cu/water ($\varphi_1 = 0$)		Al_2O_3-Cu/water ($\varphi_1 = 0.1$)	
					$Re_x^{1/2}\, C_f$	$Re_x^{-1/2} Nu_x$	$Re_x^{1/2}\, C_f$	$Re_x^{-1/2} Nu_x$
0	1	0	0	0	-1.281809	2.818154	-1.666032	3.134763
0.02	1	0	0	0	-1.415357	2.871960	-1.806661	3.198058
0.04	1	0	0	0	-1.548820	2.926740	-1.949228	3.262159
0.04	**1.5**	0	0	0	-2.845364	3.584510	-3.580961	3.995312
0.04	**2**	0	0	0	-4.380725	4.139035	-5.513250	4.613389
0.04	**2.5**	0	0	0	-6.122249	4.627582	-7.705002	5.157926
0.04	1	**-0.5**	0	0	-1.278228	1.583516	-1.618537	1.913350
0.04	1	**0**	0	0	-1.548820	2.926740	-1.949228	3.262159
0.04	1	**0.5**	0	0	-1.892721	5.005758	-2.366287	5.246558
0.04	1	0	**0.5**	0	-1.741125	2.875670	-2.212868	3.190500

0.04	1	0	**1**	0	-1.913044	2.829812	-2.446677	3.126704
0.04	1	0	**2**	0	-2.216159	2.748428	-2.856055	3.014490
0.04	1	0	0	**0.5**	-1.548820	3.572356	-1.949228	3.813774
0.04	1	0	0	**1**	-1.548820	4.067867	-1.949228	4.254325
0.04	1	0	0	**2**	-1.548820	4.814441	-1.949228	4.937795

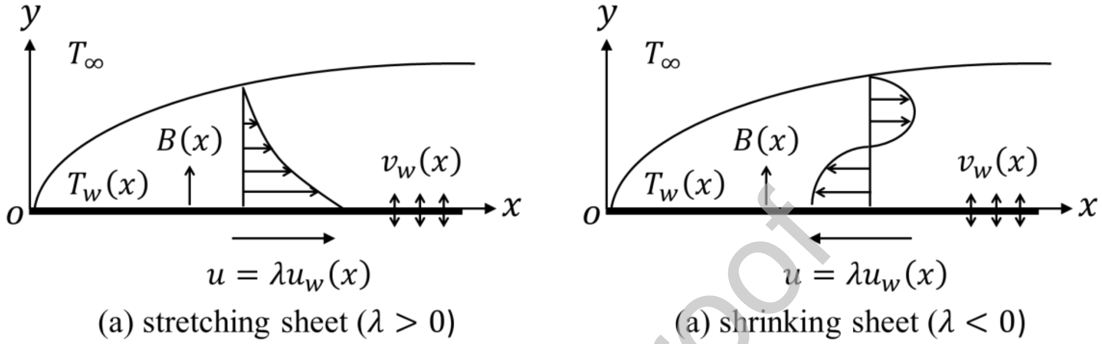

Fig. 1 Physical model

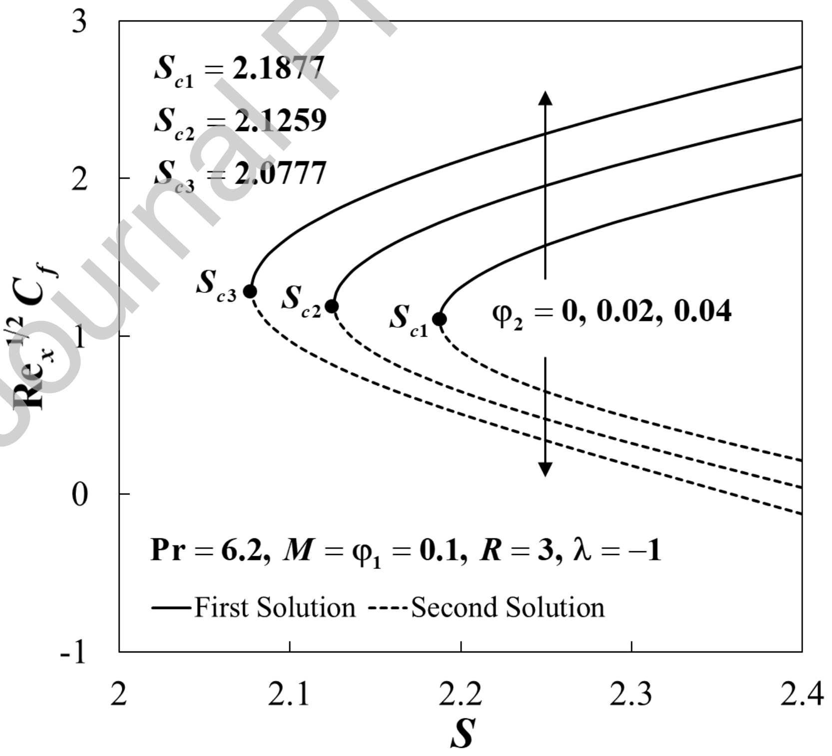

Fig. 2 Impact of φ_2 and S on $Re_x^{1/2}\ C_f$

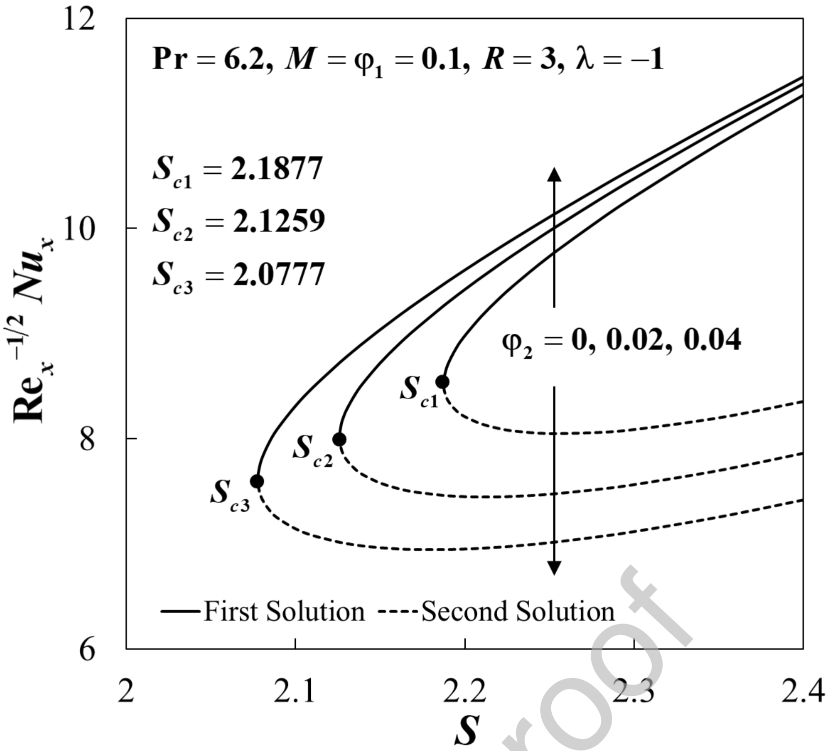

Fig. 3 Impact of φ_2 and S on $Re_x^{-1/2}Nu_x$

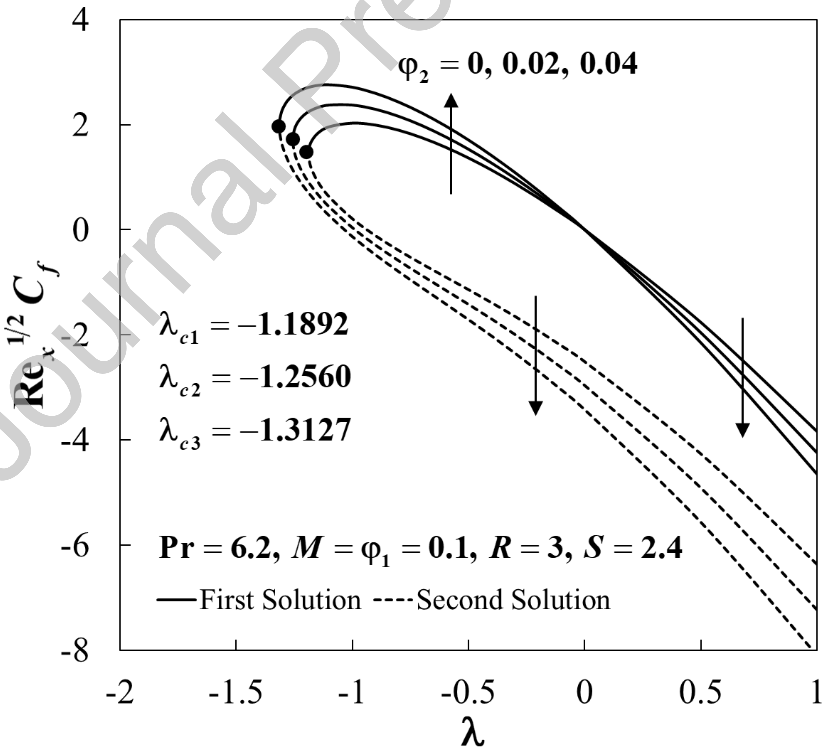

Fig. 4 Impact of φ_2 and λ on $Re_x^{1/2}\,C_f$

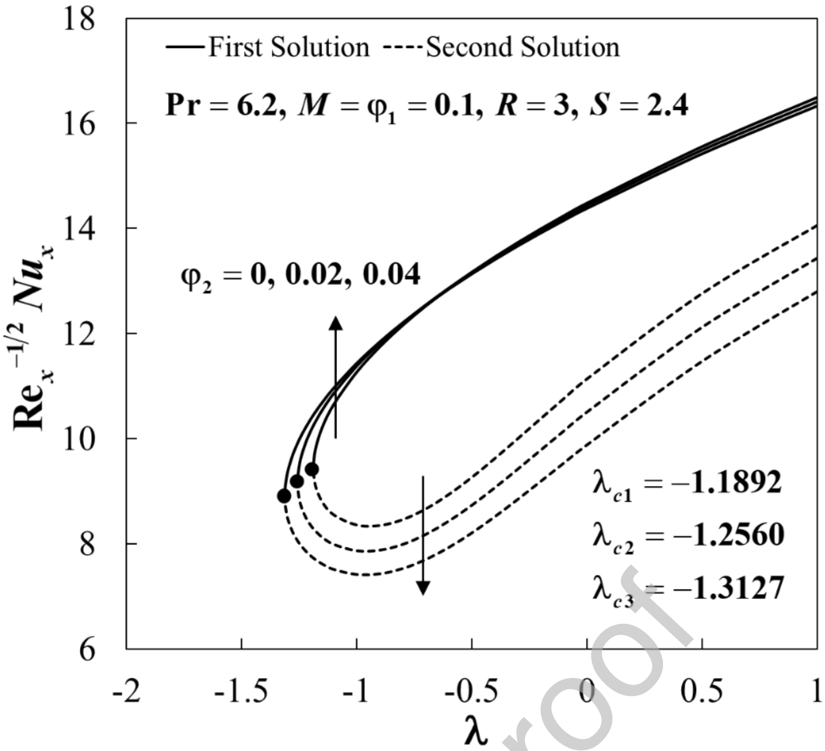

Fig. 5 Impact of φ_2 and λ on $Re_x^{-1/2}Nu_x$

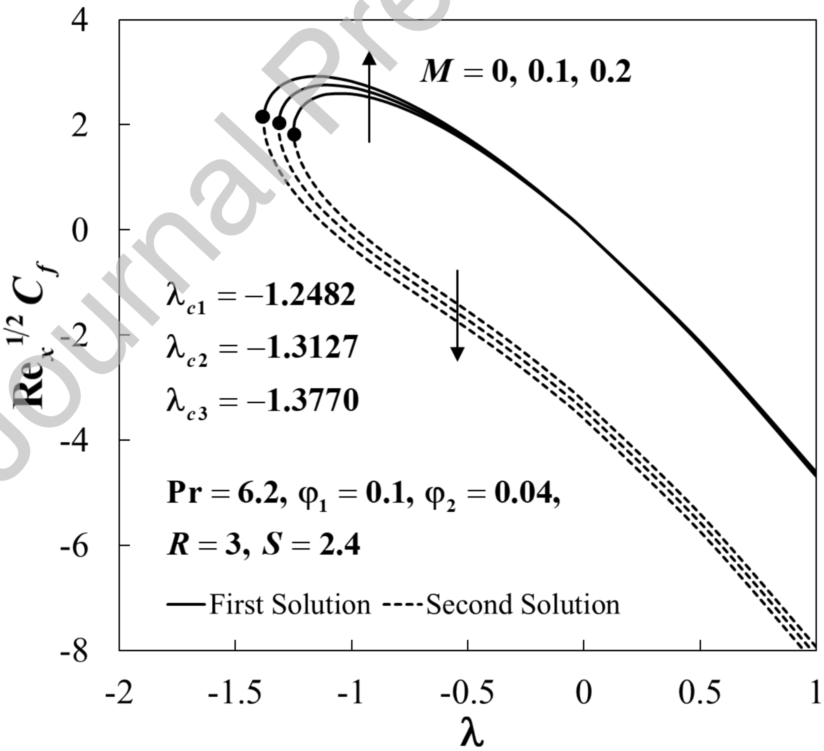

Fig. 6 Impact of M and λ on $Re_x^{1/2}\, C_f$

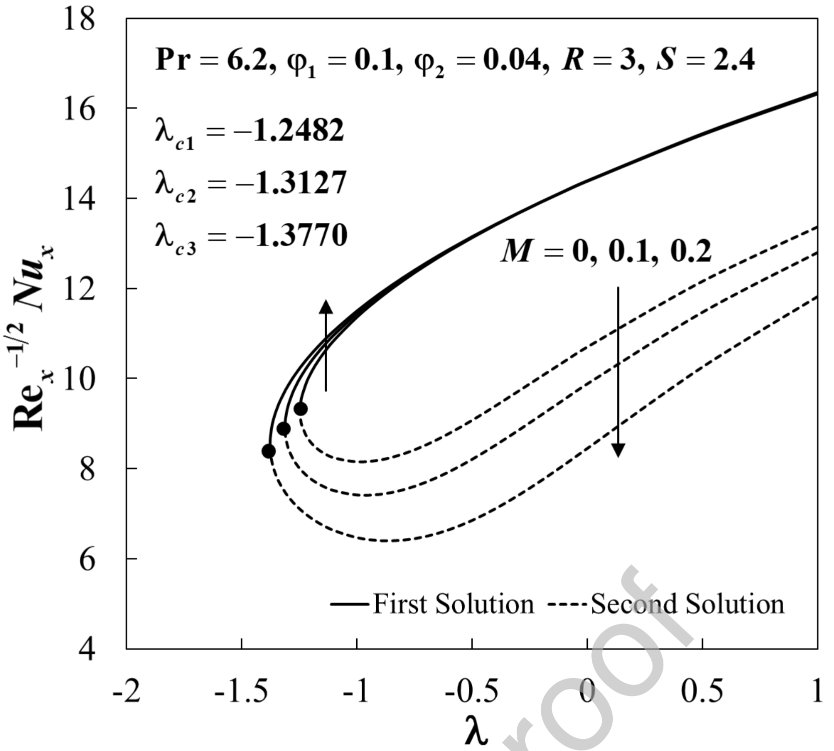

Fig. 7 Impact of M and λ on $Re_x^{-1/2}Nu_x$

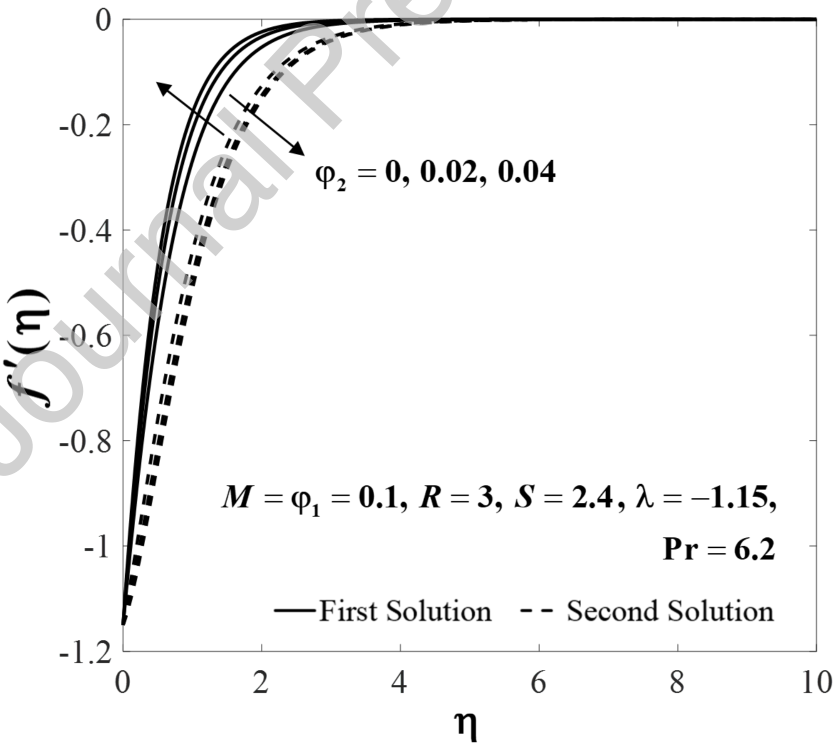

Fig. 8 Impact of φ_2 on $f'(\eta)$

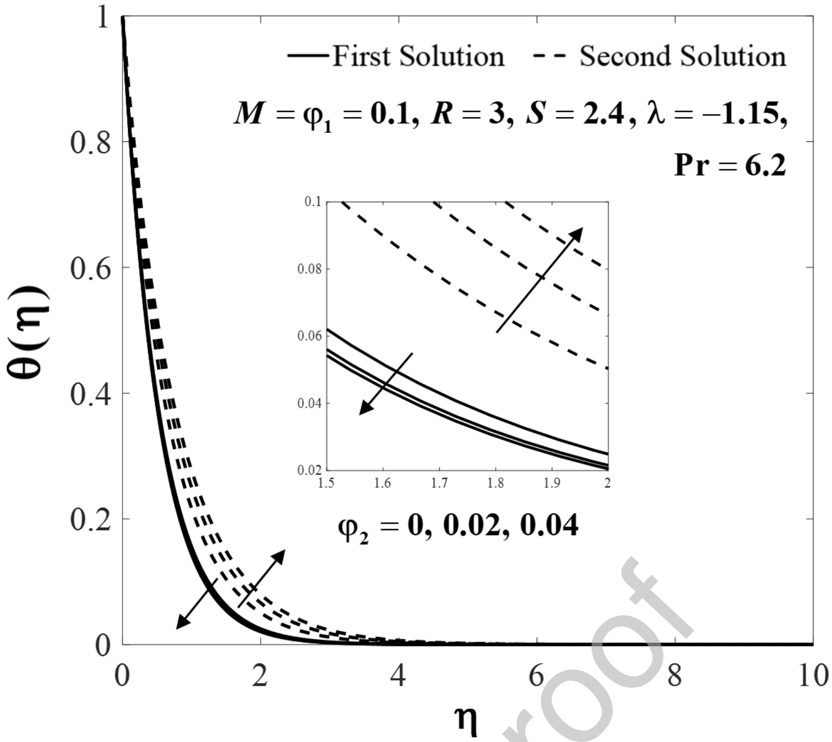

Fig. 9 Impact of φ_2 on $\theta(\eta)$

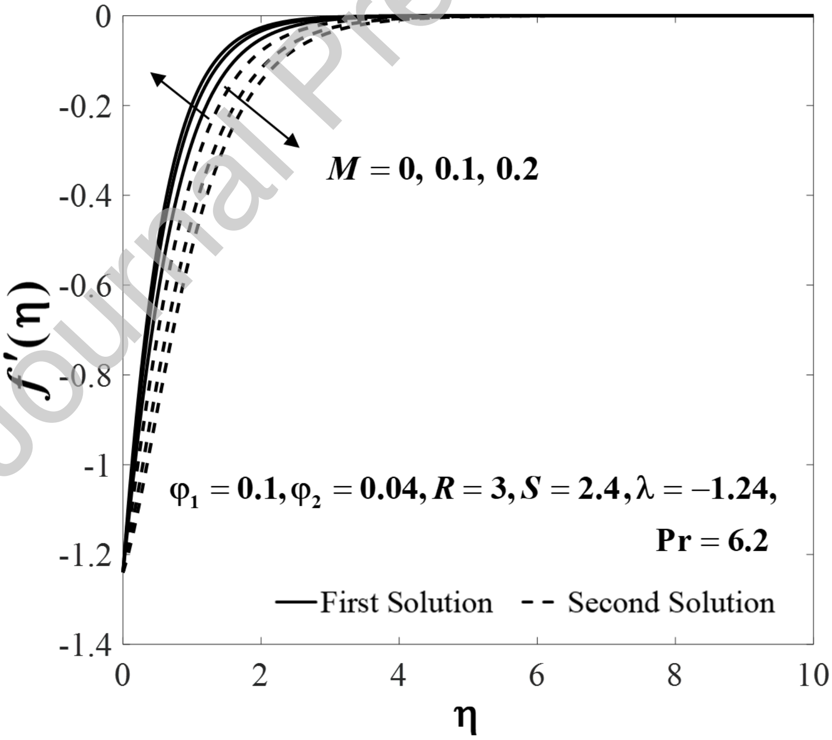

Fig. 10 Impact of M on $f'(\eta)$

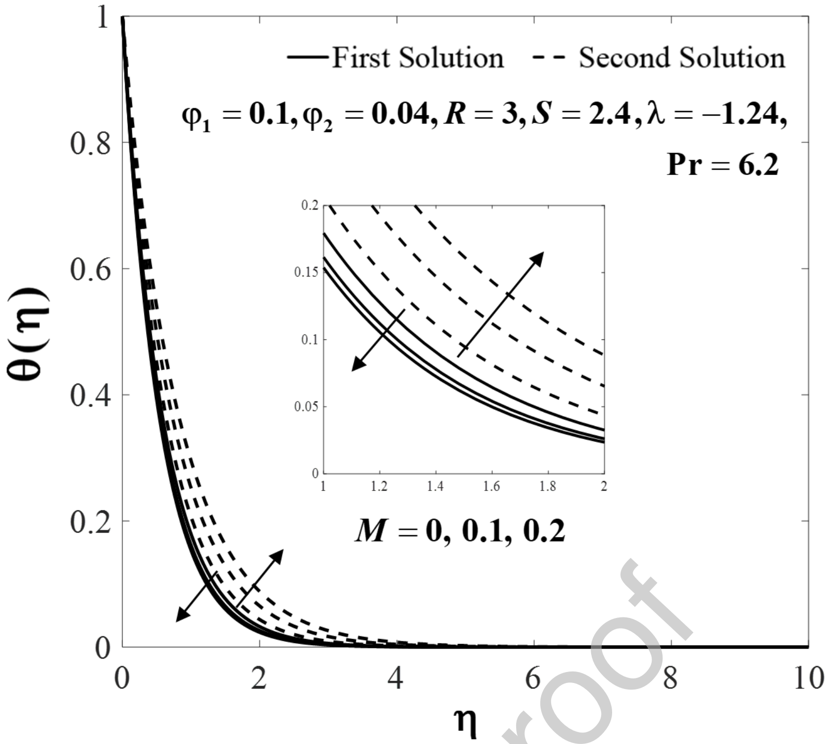

Fig. 11 Impact of M on $\theta(\eta)$

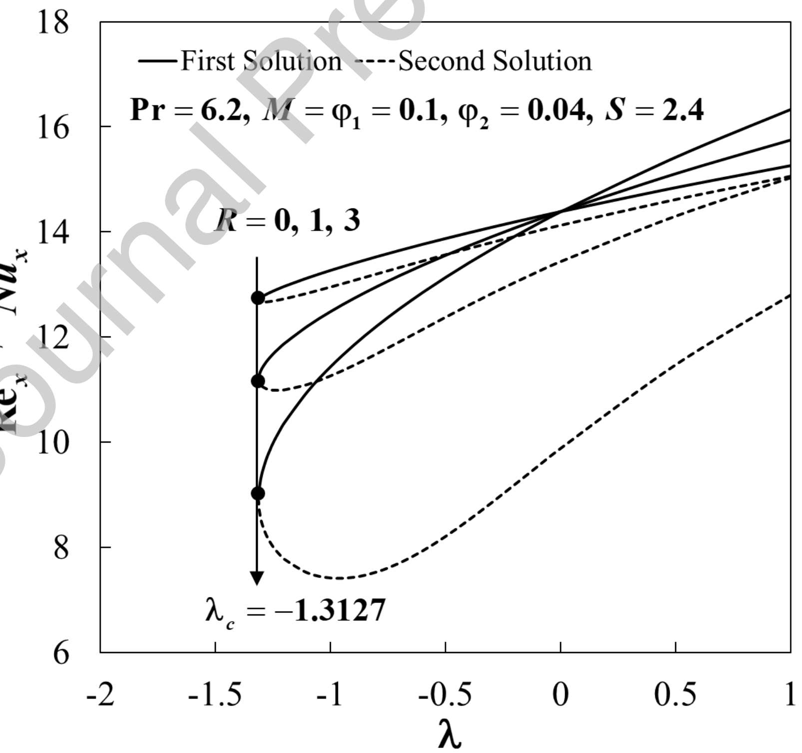

Fig. 12 Impact of R and λ on $Re_x^{-1/2} Nu_x$

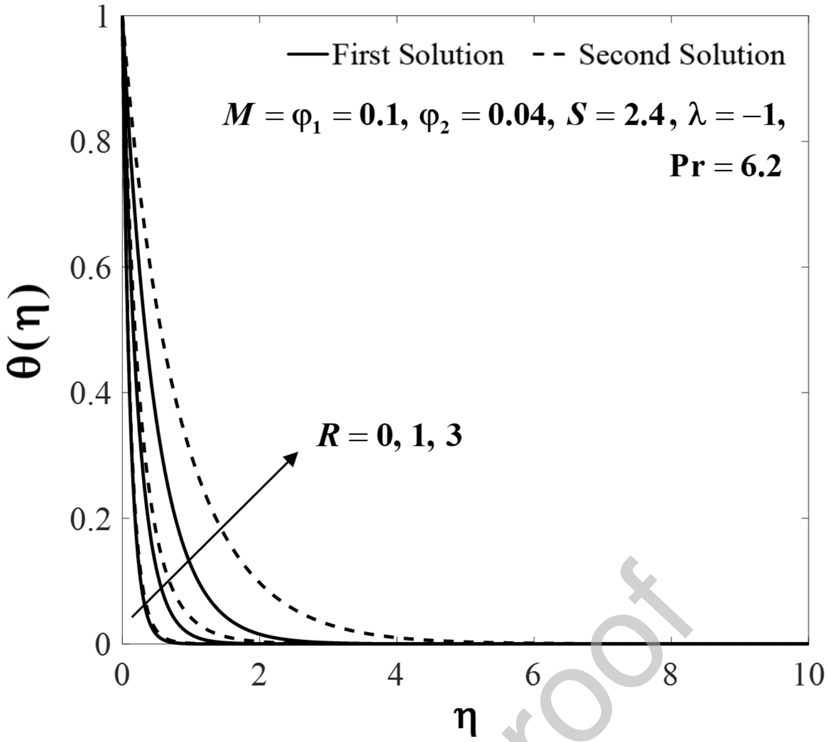

Fig. 13 Impact of R on $\theta(\eta)$

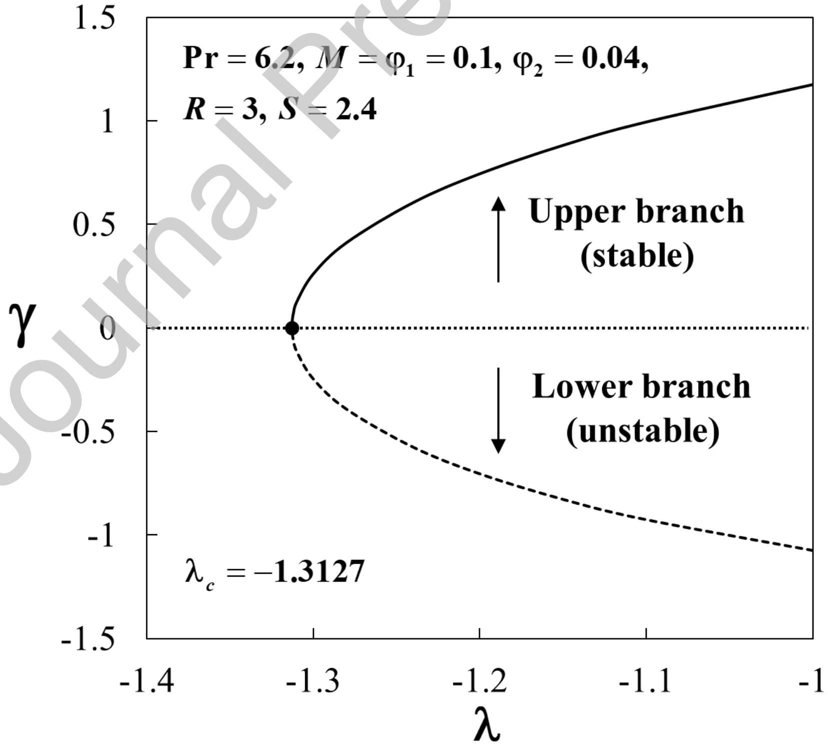

Fig. 14 The plot of the smallest eigenvalues γ against λ

Declaration of interests

The authors declare that they have no known competing financial interests or personal relationships that could have appeared to influence the work reported in this paper.

References

[1] S.U.S. Choi, J.A. Eastman, Enhancing thermal conductivity of fluids with nanoparticles, in: Proc. 1995 ASME Int. Mech. Eng. Congr. Expo., San Francisco, CA, 1995.

[2] S.K. Das, S.U.S. Choi, W. Yu, T. Pradeep, Nanofluids: Science and Technology, Wiley-Interscience, New Jersey, 2007.

[3] W.J. Minkowycz, E.M. Sparrow, J.P. Abraham, Nanoparticle heat transfer and fluid flow, CRC Press, Taylor & Fracis Group, New York, 2013.

[4] A. Shenoy, M. Sheremet, I. Pop, Convective flow and heat transfer from wavy surfaces: Viscous Fluids, Porous Media, and Nanofluids, CRC Press, Taylor and Francis Group, New York, 2016.

[5] D.A. Nield, A. Bejan, Convection in porous media, Fifth, Springer International Publishing, New York, 2017.

[6] A.A. Minea, Advances in new heat transfer fluids: From numerical to experimental techniques, CRC Press, Taylor & Fracis Group, New York, 2017.

[7] J. Buongiorno, D.C. Venerus, N. Prabhat, T. McKrell, J. Townsend, R. Christianson, Y. V. Tolmachev, P. Keblinski, L.W. Hu, J.L. Alvarado, I.C. Bang, S.W. Bishnoi, M. Bonetti, F. Botz, A. Cecere, Y. Chang, G. Chen, H. Chen, S.J. Chung, M.K. Chyu, S.K. Das, R. Di Paola, Y. Ding, F. Dubois, G. Dzido, J. Eapen, W. Escher, D. Funfschilling, Q. Galand, J. Gao, P.E. Gharagozloo, K.E. Goodson, J.G. Gutierrez, H. Hong, M. Horton, K.S. Hwang, C.S. Iorio, S.P. Jang, A.B. Jarzebski, Y. Jiang, L. Jin, S. Kabelac, A. Kamath, M.A. Kedzierski, L.G. Kieng, C. Kim, J.H. Kim, S. Kim, S.H. Lee, K.C. Leong, I. Manna, B. Michel, R. Ni, H.E. Patel, J. Philip, D. Poulikakos, C. Reynaud, R. Savino, P.K. Singh, P. Song, T. Sundararajan, E. Timofeeva, T. Tritcak, A.N. Turanov, S. Van Vaerenbergh, D. Wen, S. Witharana, C. Yang, W.H. Yeh, X.Z. Zhao, S.Q. Zhou, A benchmark study on the thermal conductivity of nanofluids, J. Appl. Phys. 106 (2009) 094312.

[8] J. Fan, L. Wang, Review of heat conduction in nanofluids, J. Heat Transfer. 133 (2011) 040801.

[9] S. Kakaç, A. Pramuanjaroenkij, Review of convective heat transfer enhancement with nanofluids, Int. J. Heat Mass Transf. 52 (2009) 3187–3196.

[10] O. Manca, Y. Jaluria, D. Poulikakos, Heat transfer in nanofluids, Adv. Mech. Eng. 2 (2010) 380826.

[11] M. Sheikholeslami, D.D. Ganji, Nanofluid convective heat transfer using semi analytical and numerical approaches: A review, J. Taiwan Inst. Chem. Eng. 65 (2016) 43–77.

[12] T.G. Myers, H. Ribera, V. Cregan, Does mathematics contribute to the nanofluid debate?, Int. J. Heat Mass Transf. 111 (2017) 279–288.

[13] O. Mahian, A. Kianifar, S.A. Kalogirou, I. Pop, S. Wongwises, A review of the applications of nanofluids in solar energy, Int. J. Heat Mass Transf. 57 (2013) 582–594.

[14] O. Mahian, L. Kolsi, M. Amani, P. Estellé, G. Ahmadi, C. Kleinstreuer, J.S. Marshall, M. Siavashi, R.A. Taylor, H. Niazmand, S. Wongwises, T. Hayat, A. Kolanjiyil, A. Kasaeian, I. Pop, Recent advances in modeling and simulation of nanofluid flows — Part I : Fundamentals and theory, Phys. Rep. 790 (2019) 1–48.

[15] O. Mahian, L. Kolsi, M. Amani, P. Estellé, G. Ahmadi, C. Kleinstreuer, J.S. Marshall, R.A. Taylor, E. Abu-nada, S. Rashidi, H. Niazmand, S. Wongwises, T. Hayat, A. Kasaeian, I. Pop, Recent advances in modeling and simulation of nanofluid flows — Part II : Applications, Phys. Rep. 791 (2019) 1–59.

[16] S. Qayyum, M.I. Khan, T. Hayat, A. Alsaedi, A framework for nonlinear thermal radiation and homogeneous-heterogeneous reactions flow based on silver-water and copper-water nanoparticles: A numerical model for probable error, Results Phys. 7 (2017) 1907–1914.

[17] M.W.A. Khan, M.I. Khan, T. Hayat, A. Alsaedi, Entropy generation minimization (EGM) of nanofluid flow by a thin moving needle with nonlinear thermal radiation, Phys. B Condens. Matter. 534 (2018) 113–119.

[18] T. Hayat, M.I. Khan, M. Farooq, A. Alsaedi, T. Yasmeen, Impact of Marangoni convection in the flow of carbon–water nanofluid with thermal radiation, Int. J. Heat Mass Transf. 106 (2017) 810–815.

[19] T. Hayat, M.I. Khan, M. Waqas, A. Alsaedi, M. Farooq, Numerical simulation for

melting heat transfer and radiation effects in stagnation point flow of carbon–water nanofluid, Comput. Methods Appl. Mech. Eng. 315 (2017) 1011–1024.

[20] T. Hayat, M.I. Khan, S. Qayyum, A. Alsaedi, Entropy generation in flow with silver and copper nanoparticles, Colloids Surfaces A Physicochem. Eng. Asp. 539 (2018) 335–346.

[21] T. Hayat, M. Waqas, M.I. Khan, A. Alsaedi, Analysis of thixotropic nanomaterial in a doubly stratified medium considering magnetic field effects, Int. J. Heat Mass Transf. 102 (2016) 1123–1129.

[22] T. Hayat, S. Qayyum, M.I. Khan, A. Alsaedi, Entropy generation in magnetohydrodynamic radiative flow due to rotating disk in presence of viscous dissipation and Joule heating, Phys. Fluids. 30 (2018) 017101.

[23] T. Hayat, M.I. Khan, M. Waqas, A. Alsaedi, Mathematical modeling of non-Newtonian fluid with chemical aspects: A new formulation and results by numerical technique, Colloids Surfaces A Physicochem. Eng. Asp. 518 (2017) 263–272.

[24] T. Hayat, M.I. Khan, M. Farooq, A. Alsaedi, M.I. Khan, Thermally stratified stretching flow with Cattaneo–Christov heat flux, Int. J. Heat Mass Transf. 106 (2017) 289–294.

[25] T. Hayat, M.I. Khan, M. Waqas, A. Alsaedi, M.I. Khan, Radiative flow of micropolar nanofluid accounting thermophoresis and Brownian moment, Int. J. Hydrogen Energy. 42 (2017) 16821–16833.

[26] T. Hayat, M.I. Khan, S. Qayyum, A. Alsaedi, M.I. Khan, New thermodynamics of entropy generation minimization with nonlinear thermal radiation and nanomaterials, Phys. Lett. Sect. A Gen. At. Solid State Phys. 382 (2018) 749–760.

[27] T. Hayat, M.I. Khan, M. Farooq, T. Yasmeen, A. Alsaedi, Stagnation point flow with Cattaneo-Christov heat flux and homogeneous-heterogeneous reactions, J. Mol. Liq. 220 (2016) 49–55.

[28] T. Hayat, M.I. Khan, M. Farooq, A. Alsaedi, M. Waqas, T. Yasmeen, Impact of Cattaneo-Christov heat flux model in flow of variable thermal conductivity fluid over a variable thicked surface, Int. J. Heat Mass Transf. 99 (2016) 702–710.

[29] T. Hayat, S. Ahmad, M.I. Khan, A. Alsaedi, Simulation of ferromagnetic nanomaterial flow of Maxwell fluid, Results Phys. 8 (2018) 34–40.

[30] M.I. Khan, M.I. Khan, M. Waqas, T. Hayat, A. Alsaedi, Chemically reactive flow of Maxwell liquid due to variable thicked surface, Int. Commun. Heat Mass Transf. 86 (2017) 231–238.

[31] M.I. Khan, T. Hayat, M.I. Khan, A. Alsaedi, A modified homogeneous-heterogeneous reactions for MHD stagnation flow with viscous dissipation and Joule heating, Int. J. Heat Mass Transf. 113 (2017) 310–317.

[32] M.I. Khan, M. Waqas, T. Hayat, A. Alsaedi, A comparative study of Casson fluid with homogeneous-heterogeneous reactions, J. Colloid Interface Sci. 498 (2017) 85–90.

[33] M.I. Khan, T. Hayat, M.I. Khan, A. Alsaedi, Activation energy impact in nonlinear radiative stagnation point flow of Cross nanofluid, Int. Commun. Heat Mass Transf. 91 (2018) 216–224.

[34] M.I. Khan, M. Waqas, T. Hayat, M.I. Khan, A. Alsaedi, Behavior of stratification phenomenon in flow of Maxwell nanomaterial with motile gyrotactic microorganisms in the presence of magnetic field, Int. J. Mech. Sci. 131–132 (2017) 426–434.

[35] M. Farooq, M.I. Khan, M. Waqas, T. Hayat, A. Alsaedi, M.I. Khan, MHD stagnation point flow of viscoelastic nanofluid with non-linear radiation effects, J. Mol. Liq. 221 (2016) 1097–1103.

[36] K.L. Hsiao, Stagnation electrical MHD nanofluid mixed convection with slip boundary on a stretching sheet, Appl. Therm. Eng. 98 (2016) 850–861.

[37] K.L. Hsiao, Combined electrical MHD heat transfer thermal extrusion system using Maxwell fluid with radiative and viscous dissipation effects, Appl. Therm. Eng. 112 (2017) 1281–1288.

[38] K.L. Hsiao, To promote radiation electrical MHD activation energy thermal extrusion manufacturing system efficiency by using Carreau-Nanofluid with parameters control method, Energy. 130 (2017) 486–499.

[39] K.L. Hsiao, Micropolar nanofluid flow with MHD and viscous dissipation effects towards a stretching sheet with multimedia feature, Int. J. Heat Mass Transf. 112 (2017) 983–990.

[40] J. Buongiorno, Convective transport in nanofluids, J. Heat Transfer. 128 (2006) 240–250.

[41] R.K. Tiwari, M.K. Das, Heat transfer augmentation in a two-sided lid-driven differentially heated square cavity utilizing nanofluids, Int. J. Heat Mass Transf. 50 (2007) 2002–2018.

[42] J. Sarkar, P. Ghosh, A. Adil, A review on hybrid nanofluids: Recent research, development and applications, Renew. Sustain. Energy Rev. 43 (2015) 164–177.

[43] M. Hemmat Esfe, A. Alirezaie, M. Rejvani, An applicable study on the thermal

conductivity of SWCNT-MgO hybrid nanofluid and price-performance analysis for energy management, Appl. Therm. Eng. 111 (2017) 1202–1210.

[44] L.S. Sundar, K.V. Sharma, M.K. Singh, A.C.M. Sousa, Hybrid nanofluids preparation, thermal properties, heat transfer and friction factor – A review, Renew. Sustain. Energy Rev. 68 (2017) 185–198.

[45] J.A.R. Babu, K.K. Kumar, S.S. Rao, State-of-art review on hybrid nanofluids, Renew. Sustain. Energy Rev. 77 (2017) 551–565.

[46] N.A.C. Sidik, I.M. Adamu, M.M. Jamil, G.H.R. Kefayati, R. Mamat, G. Najafi, Recent progress on hybrid nanofluids in heat transfer applications: A comprehensive review, Int. Commun. Heat Mass Transf. 78 (2016) 68–79.

[47] S. Akilu, K. V. Sharma, A.T. Baheta, R. Mamat, A review of thermophysical properties of water based composite nanofluids, Renew. Sustain. Energy Rev. 66 (2016) 654–678.

[48] K.Y. Leong, K.Z. Ku Ahmad, H.C. Ong, M.J. Ghazali, A. Baharum, Synthesis and thermal conductivity characteristic of hybrid nanofluids – A review, Renew. Sustain. Energy Rev. 75 (2017) 868–878.

[49] M.H. Ahmadi, A. Mirlohi, M. Alhuyi Nazari, R. Ghasempour, A review of thermal conductivity of various nanofluids, J. Mol. Liq. 265 (2018) 181–188.

[50] G. Huminic, A. Huminic, Hybrid nanofluids for heat transfer applications – A state-of-the-art review, Int. J. Heat Mass Transf. 125 (2018) 82–103.

[51] S.P.A. Devi, S.S.U. Devi, Numerical investigation of hydromagnetic hybrid Cu-Al_2O_3/water nanofluid flow over a permeable stretching sheet with suction, Int. J. Nonlinear Sci. Numer. Simul. 17 (2016) 249–257.

[52] S. Suresh, K.P. Venkitaraj, P. Selvakumar, M. Chandrasekar, Synthesis of Al_2O_3-Cu/water hybrid nanofluids using two step method and its thermo physical properties, Colloids Surfaces A Physicochem. Eng. Asp. 388 (2011) 41–48.

[53] S.S.U. Devi, S.P.A. Devi, Numerical investigation of three-dimensional hybrid Cu–Al_2O_3/water nanofluid flow over a stretching sheet with effecting Lorentz force subject to Newtonian heating, Can. J. Phys. 94 (2016) 490–496.

[54] I. Waini, A. Ishak, I. Pop, Unsteady flow and heat transfer past a stretching/shrinking sheet in a hybrid nanofluid, Int. J. Heat Mass Transf. 136 (2019) 288–297.

[55] I. Waini, A. Ishak, I. Pop, Flow and heat transfer along a permeable stretching/shrinking curved surface in a hybrid nanofluid, Phys. Scr. 94 (2019)

105219.

[56] I. Waini, A. Ishak, I. Pop, Hybrid nanofluid flow and heat transfer over a nonlinear permeable stretching/shrinking surface, Int. J. Numer. Methods Heat Fluid Flow. 29 (2019) 3110–3127.

[57] I. Waini, A. Ishak, I. Pop, Hybrid nanofluid flow and heat transfer past a vertical thin needle with prescribed surface heat flux, Int. J. Numer. Methods Heat Fluid Flow. (2019) https://doi.org/10.1108/HFF-04-2019-0277.

[58] N.S. Khashi'ie, N.M. Arifin, R. Nazar, E.H. Hafidzuddin, N. Wahi, I. Pop, Magnetohydrodynamics (MHD) axisymmetric flow and heat transfer of a hybrid nanofluid past a radially permeable stretching/shrinking sheet with Joule heating, Chinese J. Phys. (2019) https://doi.org/10.1016/j.cjph.2019.11.008.

[59] T. Hayat, S. Nadeem, Heat transfer enhancement with Ag–CuO/water hybrid nanofluid, Results Phys. 7 (2017) 2317–2324.

[60] T. Hayat, S. Nadeem, A.U. Khan, Rotating flow of Ag-CuO/H_2O hybrid nanofluid with radiation and partial slip boundary effects, Eur. Phys. J. E. 41 (2018) 75.

[61] W. Jamshed, A. Aziz, Cattaneo–Christov based study of TiO_2–CuO/EG Casson hybrid nanofluid flow over a stretching surface with entropy generation, Appl. Nanosci. 8 (2018) 685–698.

[62] M. Yousefi, S. Dinarvand, M. Eftekhari Yazdi, I. Pop, Stagnation-point flow of an aqueous titania-copper hybrid nanofluid toward a wavy cylinder, Int. J. Numer. Methods Heat Fluid Flow. 28 (2018) 1716–1735.

[63] M.N. Rostami, S. Dinarvand, I. Pop, Dual solutions for mixed convective stagnation-point flow of an aqueous silica–alumina hybrid nanofluid, Chinese J. Phys. 56 (2018) 2465–2478.

[64] S. Dinarvand, Nodal/saddle stagnation-point boundary layer flow of CuO–Ag/water hybrid nanofluid: A novel hybridity model, Microsyst. Technol. (2019) 1–15.

[65] M. Subhani, S. Nadeem, Numerical analysis of micropolar hybrid nanofluid, Appl. Nanosci. 9 (2019) 447–459.

[66] S. Ahmad Khan, M.I. Khan, T. Hayat, M. Faisal Javed, A. Alsaedi, Mixed convective non-linear radiative flow with TiO_2-Cu-water hybrid nanomaterials and induced magnetic field, Int. J. Numer. Methods Heat Fluid Flow. (2019) https://doi.org/10.1108/hff-12-2018-0748.

[67] E.H. Aly, I. Pop, MHD flow and heat transfer over a permeable stretching/shrinking

sheet in a hybrid nanofluid with a convective boundary condition, Int. J. Numer. Methods Heat Fluid Flow. (2019) https://doi.org/10.1108/hff-12-2018-0794.

[68] L.J. Crane, Flow past a stretching plate, Zeitschrift Für Angew. Math. Und Phys. ZAMP. 21 (1970) 645–647.

[69] C.Y. Wang, Liquid film on an unsteady stretching surface, Q. Appl. Math. 48 (1990) 601–610.

[70] S. Goldstein, On backward boundary layers and flow in converging passages, J. Fluid Mech. 21 (1965) 33–45.

[71] M. Miklavčič, C.Y. Wang, Viscous flow due to a shrinking sheet, Q. Appl. Math. 64 (2006) 283–290.

[72] T. Fang, Boundary layer flow over a shrinking sheet with power-law velocity, Int. J. Heat Mass Transf. 51 (2008) 5838–5843.

[73] E. Magyari, B. Keller, Heat and mass transfer in the boundary layers on an exponentially stretching continuous surface, J. Phys. D. Appl. Phys. 32 (1999) 577–585.

[74] E.M.A. Elbashbeshy, Heat transfer over an exponentially stretching continuous surface with suction, Arch. Mech. 53 (2001) 643–651.

[75] M.A. El-Aziz, Viscous dissipation effect on mixed convection flow of a micropolar fluid over an exponentially stretching sheet, Can. J. Phys. 87 (2009) 359–368.

[76] M. Sajid, T. Hayat, Influence of thermal radiation on the boundary layer flow due to an exponentially stretching sheet, Int. Commun. Heat Mass Transf. 35 (2008) 347–356.

[77] B. Bidin, R. Nazar, Numerical solution of the boundary layer flow over an exponentially stretching sheet with thermal radiation, Eur. J. Sci. Res. 33 (2009) 710–717.

[78] K. Bhattacharyya, I. Pop, MHD boundary layer flow due to an exponentially shrinking sheet, Magnetohydrodynamics. 47 (2011) 337–344.

[79] S. Nadeem, R. Ul Haq, C. Lee, MHD flow of a Casson fluid over an exponentially shrinking sheet, Sci. Iran. 19 (2012) 1550–1553.

[80] A. Ishak, MHD boundary layer flow due to an exponentially stretching sheet with radiation effect, Sains Malays. 40 (2011) 391–395.

[81] F. Mabood, W.A. Khan, A.I.M. Ismail, MHD flow over exponential radiating stretching sheet using homotopy analysis method, J. King Saud Univ. - Eng. Sci. 29 (2017) 68–74.

[82] A. Zaib, K. Bhattacharyya, S. Shafie, Unsteady boundary layer flow and heat transfer over an exponentially shrinking sheet with suction in a copper-water nanofluid, J. Cent. South Univ. 22 (2015) 4856–4863.

[83] S. Ghosh, S. Mukhopadhyay, Stability analysis for model-based study of nanofluid flow over an exponentially shrinking permeable sheet in presence of slip, Neural Comput. Appl. (2019) https://doi.org/10.1007/s00521-019-04221-w.

[84] E.H. Hafidzuddin, R. Nazar, N.M. Arifin, I. Pop, Boundary layer flow and heat transfer over a permeable exponentially stretching/shrinking sheet with generalized slip velocity, J. Appl. Fluid Mech. 9 (2016) 2025–2036.

[85] M.K. Partha, P.V.S.N. Murthy, G.P. Rajasekhar, Effect of viscous dissipation on the mixed convection heat transfer from an exponentially stretching surface, Heat Mass Transf. Und Stoffuebertragung. 41 (2005) 360–366.

[86] D. Pal, Mixed convection heat transfer in the boundary layers on an exponentially stretching surface with magnetic field, Appl. Math. Comput. 217 (2010) 2356–2369.

[87] A.M. Rohni, S. Ahmad, A.I.M. Ismail, I. Pop, Boundary layer flow and heat transfer over an exponentially shrinking vertical sheet with suction, Int. J. Therm. Sci. 64 (2013) 264–272.

[88] K. Bhattacharyya, Boundary layer flow and heat transfer over an exponentially shrinking sheet, Chinese Phys. Lett. 28 (2011) 074701.

[89] R. Sharma, A. Ishak, R. Nazar, I. Pop, Boundary layer flow and heat transfer over a permeable exponentially shrinking sheet in the presence of thermal radiation and partial slip, J. Appl. Fluid Mech. 7 (2014) 125–134.

[90] M.R. Krishnamurthy, B.C. Prasannakumara, B.J. Gireesha, S.R. Gorla, Effect of viscous dissipation on hydromagnetic fluid flow and heat transfer of nanofluid over an exponentially stretching sheet with fluid-particle suspension, Cogent Math. 2 (2015) 1050973.

[91] S. Rosseland, Astrophysik und atom-theoretische Grundlagen, Springer-Verlag, Berlin, 1931.

[92] R. Cortell, Heat and fluid flow due to non-linearly stretching surfaces, Appl. Math. Comput. 217 (2011) 7564–7572.

[93] E. Magyari, A. Pantokratoras, Note on the effect of thermal radiation in the linearized Rosseland approximation on the heat transfer characteristics of various boundary layer flows, Int. Commun. Heat Mass Transf. 38 (2011) 554–556.

[94] H.F. Oztop, E. Abu-Nada, Numerical study of natural convection in partially heated rectangular enclosures filled with nanofluids, Int. J. Heat Fluid Flow. 29 (2008) 1326–1336.

[95] J. Raza, A. Rohni, Z. Omar, Numerical investigation of copper-water (Cu-water) nanofluid with different shapes of nanoparticles in a channel with stretching wall: Slip effects, Math. Comput. Appl. 21 (2016) 43.

[96] T. Fang, J. Zhang, Closed-form exact solutions of MHD viscous flow over a shrinking sheet, Commun. Nonlinear Sci. Numer. Simul. 14 (2009) 2853–2857.

[97] J.H. Merkin, On dual solutions occurring in mixed convection in a porous medium, J. Eng. Math. 20 (1986) 171–179.

[98] P.D. Weidman, D.G. Kubitschek, A.M.J. Davis, The effect of transpiration on self-similar boundary layer flow over moving surfaces, Int. J. Eng. Sci. 44 (2006) 730–737.

[99] S.D. Harris, D.B. Ingham, I. Pop, Mixed convection boundary-layer flow near the stagnation point on a vertical surface in a porous medium: Brinkman model with slip, Transp. Porous Media. 77 (2009) 267–285.

[100] L.F. Shampine, I. Gladwell, S. Thompson, Solving ODEs with MATLAB, Cambridge University Press, Cambridge, 2003.

[101] I.S. Awaludin, A. Ishak, I. Pop, On the stability of MHD boundary layer flow over a stretching/shrinking wedge, Sci. Rep. 8 (2018) 13622.

[102] S.K. Soid, A. Ishak, I. Pop, MHD stagnation-point flow over a stretching/shrinking sheet in a micropolar fluid with a slip boundary, Sains Malays. 47 (2018) 2907–2916.

[103] R. Jusoh, R. Nazar, I. Pop, Magnetohydrodynamic boundary layer flow and heat transfer of nanofluids past a bidirectional exponential permeable stretching/shrinking sheet with viscous dissipation effect, J. Heat Transfer. 141 (2019) 012406.

[104] F. Kamal, K. Zaimi, A. Ishak, I. Pop, Stability analysis of MHD Stagnation-point flow towards a permeable stretching/shrinking sheet in a nanofluid with chemical reactions effect, Sains Malays. 48 (2019) 243–250.

[105] N.S. Khashi'ie, N.M. Arifin, R. Nazar, E.H. Hafidzuddin, N. Wahi, I. Pop, A stability analysis for magnetohydrodynamics stagnation point flow with zero nanoparticles flux condition and anisotropic slip, Energies. 12 (2019) 1268.

[106] N.S. Khashi'ie, N.M. Arifin, M.M. Rashidi, E.H. Hafidzuddin, N. Wahi, Magnetohydrodynamics (MHD) stagnation point flow past a shrinking/stretching surface with double stratification effect in a porous medium, J. Therm. Anal. Calorim.

8 (2019) 1–14.

[107] I. Waini, A. Ishak, I. Pop, On the stability of the flow and heat transfer over a moving thin needle with prescribed surface heat flux, Chinese J. Phys. 60 (2019) 651–658.

Nomenclature

T_0, U_0	constant
B_0	uniform magnetic strength
C_f	skin friction coefficient
C_p	specific heat at constant pressure ($Jkg^{-1}K^{-1}$)
(ρC_p)	heat capacitance of the fluid ($JK^{-1}m^{-3}$)
$f(\eta)$	dimensionless stream function
k	thermal conductivity of the fluid ($Wm^{-1}K^{-1}$)
$k*$	Rosseland mean absorption coefficient (m^{-1})
L	characteristic length of the sheet
Nu_x	local Nusselt number
M	magnetic parameter ($2\sigma_f B_0^2 L/U_0\rho_f$)
Pr	Prandtl number ($\mu_f(C_p)_f/k_f$)
q_r	radiative heat flux in y direction (Wm^{-2})
q_w	surface heat flux (Wm^{-2})
R	radiation parameter ($4\,\sigma^* T_\infty^3/k^* k_f$)
Re_x	local Reynolds number
S	mass flux parameter ($-v_w/\sqrt{U_0\nu_f/2L}\,e^{x/2L}$)
t	time (s)
T	fluid temperature (K)
T_w	surface temperature (K)
T_∞	ambient temperature (K)
u, v	velocity component in the x- and y- directions (ms^{-1})
u_w	velocity of the sheet (ms^{-1})
v_w	velocity of the mass flux (ms^{-1})
x, y	Cartesian coordinates (m)

Greek symbols

γ	eigenvalue
η	similarity variable
θ	dimensionless temperature
λ	stretching/shrinking parameter
μ	dynamic viscosity of the fluid ($kgm^{-1}s^{-1}$)
ν	kinematic viscosity of the fluid (m^2s^{-1})
ρ	density of the fluid (kgm^{-3})
σ	electrical conductivity of the fluid (Sm^{-1})
$\sigma *$	Stefan-Boltzmann constant ($Wm^{-2}K^{-4}$)
τ	dimensionless time variable
τ_w	wall shear stress ($kgm^{-1}s^{-2}$)
φ_1	nanoparticle volume fractions for Al_2O_3 (alumina)
φ_2	nanoparticle volume fractions for Cu (copper)
ψ	stream function

Subscripts

f	base fluid
nf	nanofluid
hnf	hybrid nanofluid
$n1$	solid component for Al_2O_3 (alumina)
$n2$	solid component for Cu (copper)

Superscript

$'$	differentiation with respect to η